Available online at www.sciencedirect.com

ScienceDirect

Energy Procedia 114 (2017) 627 – 635

Energy Procedia

13th International Conference on Greenhouse Gas Control Technologies, GHGT-13, 14-18 November 2016, Lausanne, Switzerland

Influence of functionalized nanoparticles on the CO_2/N_2 separation properties of PVA-based gas separation membranes

Gabriel Guerrero[a], Davide Venturi[b], Thijs Peters[c], Nicolas Rival[c], Christelle Denonville[c], Christian Simon[c], Partow P. Henriksen[c], May-Britt Hägg[a,*]

[a] Department of Chemical Engineering, Norwegian University of Science and Technology, Trondheim, Norway
[b] Department of Civil, Chemical, Environmental and Materials Engineering, University of Bologna, Italy
[c] SINTEF Materials and Chemistry, Oslo, Norway

Abstract

This work investigated the influence of amino-functionalized polyhedral oligomeric silsesquioxane (amine-POSS®) nanoparticles dispersed in a polyvinyl alcohol (PVA) matrix applied as a CO_2-selective gas separation membrane. The nanoparticles belong to a class of highly branched nanosized polymers, so called POSS®. To improve the mechanical stability of the thin selective layer, the PVA-POSS® nanocomposite was deposited onto a polysulfone (PSf) support material. The influence of the ratio between PVA and amine-POSS® on the CO_2 permeance and CO_2/N_2 selectivity, the effect of the degree of humidity of the feed gas, and the stability of the obtained hybrid membranes for a total period of 1000h during exposure to SO_2 at concentrations of up to 400 ppm were investigated.

Peer-review under responsibility of the organizing committee of GHGT-13.

Keywords: Facilitated Transport Membranes (FTM), CO_2 separation, POSS®, PVA-based, fuctionalized nanoparticles.

1. Introduction

One of the long term policy goals of the EU is an 80% overall reduction of greenhouse gas emissions by 2050 [1]. It has also been accepted that fossil fuels will continue to play a key role in Europe as a fuel and as feedstock for industrial processes. To reach the demanding emission reduction target, the application of Carbon Capture and Storage (CCS) is thus a prime requirement. While solvent-based CO_2 capture is the most mature and demonstrated technology for CO_2 capture, other emerging technologies such as membranes, cryogenic separation, precipitating solvents, and sorbents may have the potential to significantly reduce costs. Among these emerging technologies, membrane-based CO_2 capture is regarded as one of the most advanced and promising options [2]. Gas separation membranes play a constantly increasing role in CO_2 separation processes, mainly due to various advantages offered, such as no chemicals needed for the separation, smaller footprint and being a modular technology compared to more traditional technologies [3-5]. The modularity and easy scale-up open chances for retrofitting of existing plants as well as flexibility with respect to the CO_2 capture rate. The technology is currently in a small-scale demonstration phase (20 TPD scale demonstration of the MTR membrane technology at the NCCC, and two small pilot demonstrations in Norway) [6].

* Corresponding author. Tel.: +47 735 94 033; +47 930 80 834
E-mail address: may-britt.hagg@ntnu.no

Peer-review under responsibility of the organizing committee of GHGT-13.
doi:10.1016/j.egypro.2017.03.1205

The efficiency of the membrane itself is the key factor in determining the advantageous nature of the process. In particular, the main parameters taken into consideration during membrane development are permeability and selectivity of the material [7]. Though tremendous improvements have been achieved in tailoring polymer structure to enhance separation properties during the last two decades, standard membrane systems always show a trade-off between permeability and selectivity, the so-called Robeson trade-off line [8]. Mixed matrix membranes (MMMs), where inorganic fillers are dispersed at a nanometre scale in a polymer matrix, or facilitated transport membranes (FTM) have been identified to potentially provide a solution to the trade-off issues of the polymeric membrane. Since the pioneering literature by Zimmerman [9], several significant review papers on the prospects of MMMs as well as the research reports on the capability of MMMs as alternative membrane materials for separation processes have been published [10, 11]. During the last decades, fillers such as zeolites, carbon molecular sieves, nano-sized inorganic particles like silica and TiO_2 or specific organic compounds like polyethylene glycol have been used in different polymeric matrices to develop new MMMs and improve their permeation properties.

Depending on the properties of the filler material, the gas transport properties can be enhanced in several ways. The incorporated filler particles could modify the properties of the continuous polymeric phase, altering the overall transport properties. This effect is significant for CO_2-inert particles that are well distributed within the polymer matrix, where the fractional free volume can be greatly modified, especially for glassy polymers. It is also well known that the presence of filler particles may alter the packing, dynamics or conformation of polymer chains near its surface, and impart great effect on the transport of large penetrates relative to small ones [12]. Chemical modification of inorganic fillers has likewise been used in order to improve not only their dispersion, but also the separation properties through the integration of functionalised nanoparticles that exhibit facilitated transport properties [13]. Among the vast field of membrane separation, a growing interest has been dedicated to these Facilitated Transport Membranes (FTMs) [13]. These materials have shown high potential in increasing both permeability and selectivity at the same time, reaching performances exceeding the Robeson upper bound for CO_2/N_2 separation. FTMs rely on the presence of a complexing agent as a CO_2 carrier in the polymeric matrix, which is capable of reacting reversibly with a particular component in the feed gas stream, Equation (1).

$$Component\ (A) + Carrier\ (C) \Leftrightarrow\ AC \tag{1}$$

Because of this additional mechanism, the total transport flux of the chosen compound (CO_2 here) can be expressed as the sum of both the Fickian diffusion and the carrier mediated diffusion, Equation (2).

$$J_A = -D_a \frac{d\,C_A}{dx} = \frac{D_A}{dx}\left(C_{A,f} - C_{A,p}\right) + \frac{D_{AC}}{dx}\left(C_{AC,f} - C_{AC,p}\right) \tag{2}$$

In the present work, we have incorporated amine-POSS® nanoparticles in PVA-based gas separation membranes in an effort to improve the CO_2/N_2 separation properties. In PVA-amine-POSS® hybrid membranes, the amine groups on the nanoparticles act as carrier for carbon dioxide. The influence of the relative humidity and the water content within the matrix is evident when the set of reactions occurring in the membrane is observed (Equation (3)-(6)) [14]:

$$CO_2 + H_2O \longrightarrow H_2CO_3 \tag{3}$$
$$H_2CO_3 + NH_2 \longrightarrow HCO_3^- + NH_3^+ \tag{4}$$
$$HCO_3^- + NH_3^+ \longrightarrow H_2CO_3 + NH_2 \tag{5}$$
$$H_2CO_3 \longrightarrow CO_2 + H_2O \tag{6}$$

Reaction (3) and (4) occur on the upstream side of the membrane, allowing the carbon dioxide to form a hydrogen carbonate ion, which is transported through the membrane and is reverted back into CO_2 at the downstream side, following Equation (5) and (6). The main scope of the current work was to evaluate the influence of the ratio between PVA and POSS on the CO_2 permeance and CO_2/N_2 selectivity. In addition, the effect of the degree of humidity of the feed gas stream were investigated. Moreover, the stability of the obtained membranes were investigated for a total period of 1000h during exposure to SO_2 at concentrations of up to 400 ppm.

2. Description of nanoparticle development

2.1. Amino-functionalized polyhedral oligomeric silsesquioxane (amine-POSS®) particles

Amine-POSS® nanoparticles were prepared by a controlled sol-gel process through the hydrolysis of 3-aminopropyltriethoxysilane (APS) (Fig. 1). The hydrolysis produces different cage structures and the amine-POSS® nanoparticles produced were therefore composed of a mixture of structures, described as T for fully condensed cage structures and by the number of silicon atoms in the cage, T_8, T_{10} and T_{12} (Fig. 2) [15]. As nanotechnology enables to obtain materials with high specific area (and hence high reactivity), our effort has been focused on optimizing the synthesis of nanoparticles with a narrow size distribution.

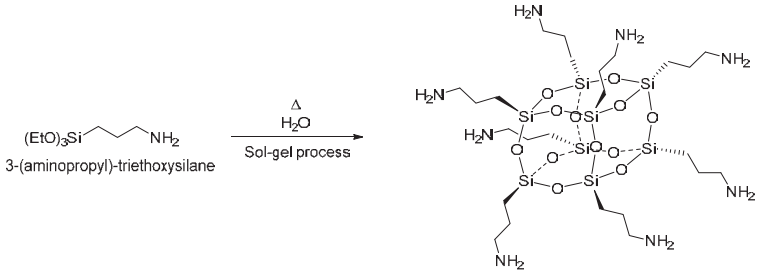

Fig. 1. Hydrolysis of APS leading to cage structures composing amine-POSS®.

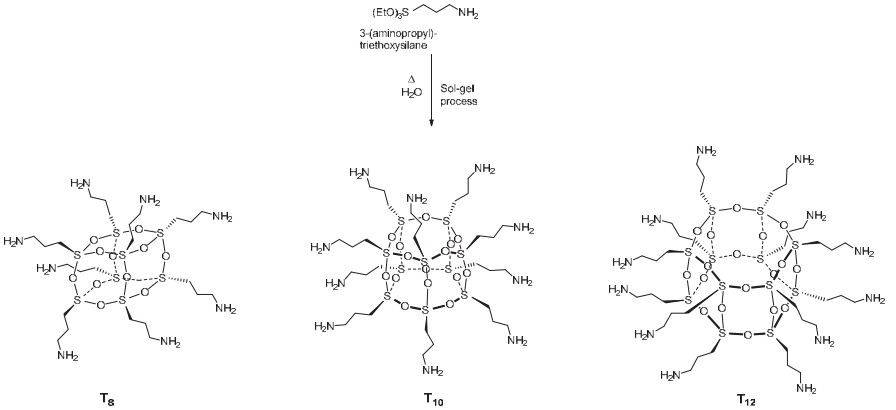

Fig. 2. Main structures composing amine-POSS®: T8, T10, T12.

Moreover, a variety of chemical surface functionalities can be obtained on the nanoparticles to provide improved or entirely new properties to the polymer matrix. A further modification of the surface groups could, for example, be applied to increase the compatibility between the hybrid nanoparticles and the polymer. In the current study, we have used fully-amine terminated polyhedral oligomeric silsesquioxane nanoparticles.

3. Preparation of the hybrid membranes

3.1. Materials

Polyvinyl alcohol (PVA) with a molecular weight of 89000-99000 (87-89% hydrolysed) supplied by Sigma Aldrich was used to prepare a 10 wt% stock solution. Polysulfone (PSf) membrane supports with MWCO 20,000 were purchased at Alfa Laval. Amine-POSS® was synthesized according to a procedure described elsewhere [15]. A solution containing 51.6 wt% nanoparticles in 2-butoxyethanol as a solvent was produced.

3.2. Membrane preparation

PVA-amine-POSS® membranes with varying amine-POSS® content, including a blank sample of pure PVA, were prepared by dip coating the flat PSf supports into a PVA-amine-POSS® solution. The PSf support was masked with alumina tape and further taped to a glass plate. Afterwards, it was dipped and left soaking in deionized water for 1 hour in order to remove the protective film. After soaking, the support was immersed for 30s vertically in a coating bath containing the PVA-amine-POSS® solution and left for 1 hour on an inclined plane, in an almost vertical position, to let the excess solution flow away by gravity. To finish the drying process, the membrane was heated in a ventilated oven for 1 hour at 90 °C. This overall procedure was repeated by turning the support upside down, in order to even out the thickness of the casted film.

The PVA-amine-POSS® dip coat solutions were prepared by weighing firstly a PVA stock solution at 10 wt.%, followed by adding deionized water to dilute the mixture and finally adding amine-POSS® dropwise. The PVA stock solution of 10 wt.% PVA in water was prepared by reflux for 7 hours at 90 °C. Quantities of the various components were calculated to achieve an overall solid concentration (PVA+amine-POSS®) of 1 wt.% and a PVA:amine-POSS® weight ratio of 1:0 (Pure PVA blank), 1:0.05, 1:0.1, 1:0.2, 1:0.4, 1:0.8. The mixtures were stirred at 500 rpm for 2 hours to achieve good homogenization of the components. While stirring, the pH of the solutions was adjusted to 12 by adding dropwise a NaOH 1 M solution until the desired value was reached. All the solutions were then filtered using a 5 μm syringe filter. To ensure a complete homogenization, the mixtures were left rolling overnight.

3.3. Scanning Electron Microscopy (SEM)

The thickness and morphology of the different membrane layers were characterised by scanning electron microscopy (SEM) using a Hitachi TM3030Plus microscope. Samples were sputtered with a thin layer of gold. Cross-section samples were obtained by fracturing at cryogenic temperature in a bath of liquid nitrogen.

3.4. Mixed Gas Permeation Test

To evaluate the CO_2 permeance and CO_2/N_2 selectivity of the prepared membranes, a mixed gas permeation setup as illustrated in Fig. 3 was used. A premixed mixture of CO_2 (10 vol%) and N_2 (90 vol%) was used as feed and was kept at an absolute pressure of 1.1-1.2 bar, while the sweep gas consisted of pure CH_4 at 1 bar. The temperature was kept constant at 25 °C. The membrane sample was cut in a disc of 50 mm in diameter and placed inside a flat sheet module. The feed and sweep gas streams were humidified through a bubbler filled with deionized water (1); in order to prevent droplets in gas streams, water traps (2) were placed before and after the feed stream. The degree of humidity of the feed gas was regulated through a dry bypass stream, fitted with a control valve (V4). Each membrane was tested at three different humidity levels (RH): 100 %, 75 % and 50 %. To equilibrate the relative humidity in the system, a feed stream of CO_2 was flowing overnight at the RH corresponding to the test performed the day after. In the permeation setup, the feed and sweep streams were regulated by two flow-meters, controlled by a computer software (LabView), which also monitor the pressure of the retentate and permeate. The volumetric flow rate of the permeate and retentate streams was measured by two bubbling columns placed at the end of the setup. For compositional analysis, the permeate stream was sent to an online gas chromatograph equipped with a thermal conductivity detector (MicroGC 3000).

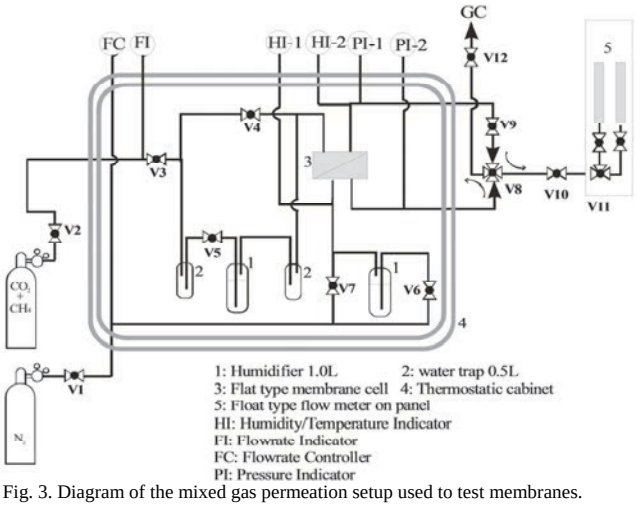

Fig. 3. Diagram of the mixed gas permeation setup used to test membranes.

Permeance of CO_2 and N_2 [m^3(STP)/(m^2 h bar)] was calculated as the gas flux through the membrane divided by the difference in partial pressure between the upstream and downstream side. The selectivity was defined as ratio between the permeance of CO_2 and the permeance of N_2 Equation (7):

$$\alpha = \frac{P_{CO_2}}{P_{N_2}} \tag{7}$$

3.5. Durability towards SO_2

The membrane durability towards SO_2 was investigated over a period of 1500 hours under varying SO_2 levels of up to 400 ppm at atmospheric pressure at a temperature of 25 °C and applying a feed composition of N_2:O_2:CO_2 of 80:5:15. A schematic representation of the applied test set-up is presented in Fig. 4. On the left side, several flow controllers were used to control the gas supply to the membrane module. Starting at a total feed flow rate of 200 NmL·min^{-1}, the SO_2 exposure was initiated by simply exchanging a part of N_2 with SO_2 in N_2 (4000 ppm – AGA AS). In this way, the feed CO_2 concentration was kept at 15%. The flow rates of the mass flow controller for N_2 and SO_2/N_2 were adjusted to obtain the SO_2 concentration needed. A sweep flow of 25 NmL·min^{-1} of Ar (99.999%) was applied at the permeate side. As during the CO_2/N_2 separation experiments, the feed and permeate gas was humidified (90-100% RH) before it entered the membrane module.

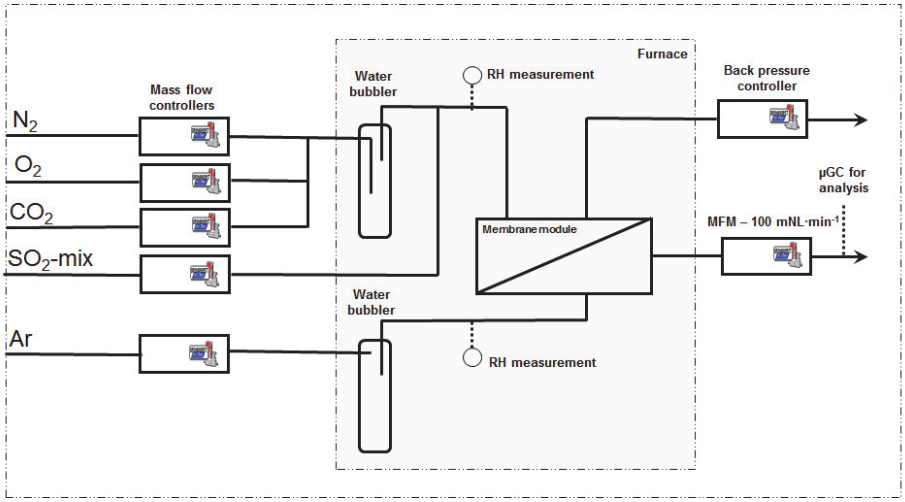

Fig. 4. Schematic representation of the set-up used to investigate the membrane durability towards SO_2.

4. Results and discussion

4.1. Nanoparticle development

The nanoparticle size distribution of basic amine-POSS® particles, prepared by a standard recipe [15], was characterised by Dynamic light scattering (DLS) using a Malvern NanoZS. Fig. 5. shows a mean particle size of 3 nm with a particle size distribution ranging from 1 to 9 nm.

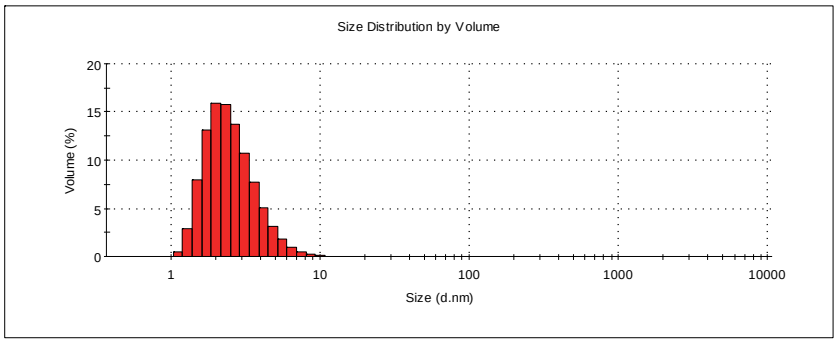

Fig. 5. Particle size distribution of basic amine-POSS® particles.

4.2. Membrane preparation and performance testing

SEM microscopy of the cross-section of the hybrid membrane revealed a homogeneous coating of the PSf support with an overall thickness of the PVA selective layer of around 3 µm, with some small variations, as presented in Fig. 6.

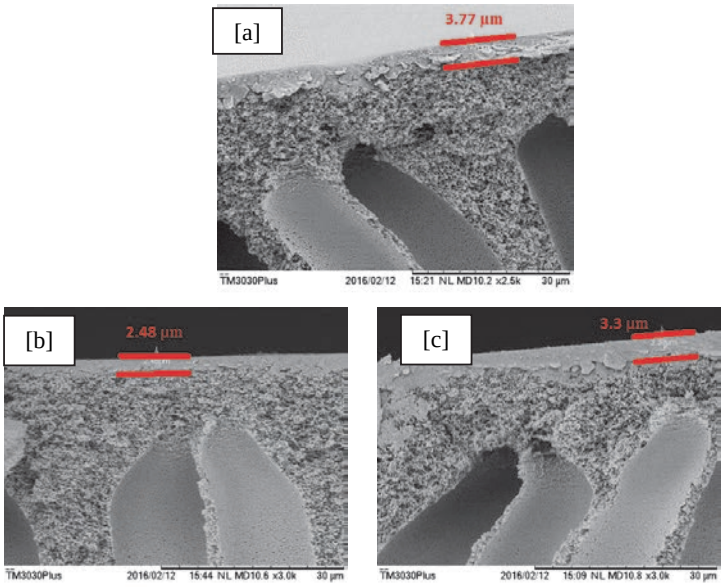

Fig. 6. SEM micrographs of the cross section of the membranes prepared: a) Pure PVA, b) PVA:amine-POSS® 1:0.05 and c) PVA:amine-POSS® 1:0.1.

Mixed gas permeation tests were performed in order to investigate the behaviour of the membranes as a function of the loading of nanoparticles and the degree of humidity of the feed gas mixture. This last variable in particular is known to significantly affect the transport properties of hydrophilic polymers, such as polyvinylalcohol and polyvinylamine [16]. In addition, the purpose of these tests focused on evaluating a possible positive effect, given by the introduction of amine-functionalized nanoparticles. In particular, the correlation between the nanoparticles content and the permeance was investigated.

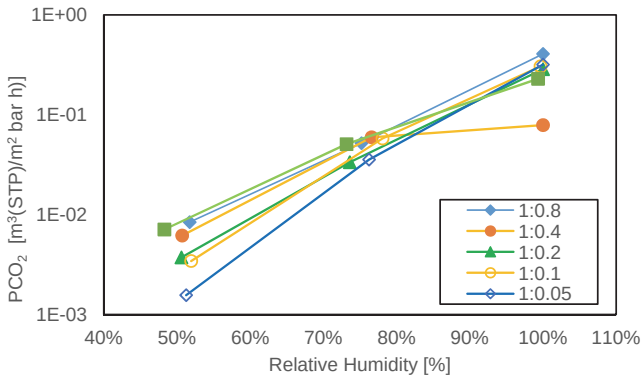

Fig. 7. CO_2 permeance of PVA-aminePOSS® blends at different relative humidity.
The nanoparticle loading of each membrane is expressed as PVA:amine-POSS® ratio.

Fig. 7 presents the CO_2 permeance of the membranes prepared as a function of the relative feed gas humidity. As expected, the feed humidity strongly influences the obtained CO_2 permeance; the permeance increases by roughly one order of magnitude at each increment of 25 percentage points in RH. This behaviour is typical for highly hydrophilic matrixes, reminding that permeability is the product of solubility (S) and diffusivity (D) of the gas species, as considered in Equation (8):

$$P = S * D \tag{8}$$

For this class of membranes, the controlling factor for permeation is usually represented by the gas solubility in the membrane. Since carbon dioxide has both the lowest kinetic diameter and the highest condensability compared to nitrogen, its permeability will always be higher than the second gas in these type of materials [17]. By increasing the relative humidity, the swelling of PVA will increase. CO_2 has a much higher solubility in water than N_2. For this reason, and for the expected contribution of the

indicated reactions 3-6 taking place at the amine-POSS® groups in presence of water, the permeance of CO_2 will increase. However, with the results obtained, it is difficult to demonstrate a facilitated transport due to the presence of the amine-POSS® particles. In Fig. 7, the point corresponding to the membrane with a PVA:amine-POSS® weight ratio of 1:0.4 at 100 RH% is a clear outlier. For this reason, this point is not taken into consideration in the following analysis.

Fig. 8 shows the CO_2 permeance and the CO_2/N_2 selectivity obtained at different feed humidity levels as a function of the nanoparticle content. Due to the fact that the nitrogen permeance at 50 RH% is very close to the detection limit of the applied GC, it was not possible to evaluate the CO_2/N_2 selectivity at this level. From these charts, it can be noted how the selectivity is highly influenced by relative humidity: at 75 RH%, it is clearly higher, reaching values up to 120, while at 100 RH%, it is limited around 60. For both humidity levels, the selectivity increases when amine-POSS® is introduced in the system, but a further increase in the amine-POSS® content does not influence the CO_2/N_2 selectivity or even has a negative effect. In particular, at 75 RH%, the selectivity increases from 51 of pure PVA to 120 of the blend with 5 wt.% of amine-POSS®. At higher amine-POSS® content, the selectivity firstly remains relatively constant, but finally drops to a selectivity value of around 85 at even higher amine-POSS® loading.

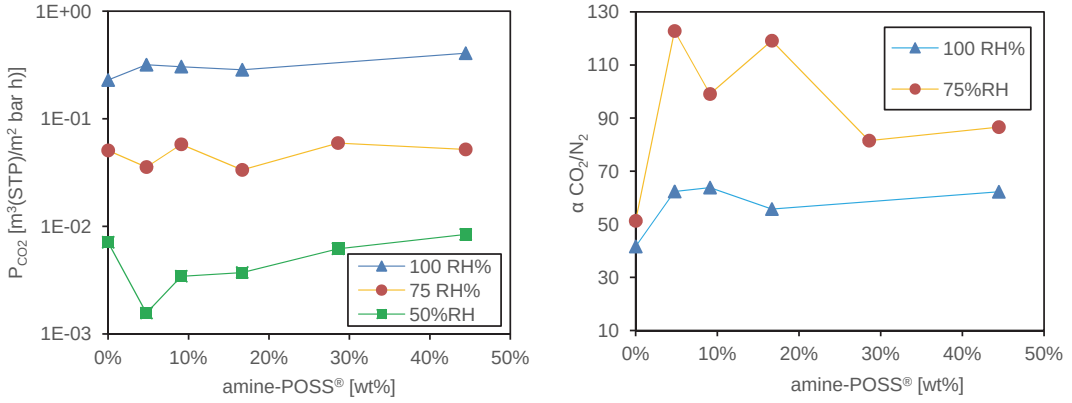

Fig. 8. CO_2 permeance (left) and CO_2/N_2 selectivity (right) at different degrees of humidity expressed as a function of amine-POSS® content.

In order to better visualize the behaviour of CO_2 permeance, Fig. 9 shows separately the data obtained at a RH of 100 and 75%, respectively. At low humidity, the permeance does not appear to be significantly influenced by the content of the amine-functionalized nanoparticles, with values constantly oscillating between 0.04 and 0.06 $m^3(STP)/(m^2\ h\ bar)$. On the other hand, the behaviour of the membranes at high humidity is more encouraging: starting from a value for pure PVA of 0.22, the permeance increases, with some oscillations, up to 0.4 $m^3(STP)/(m^2\ h\ bar)$.

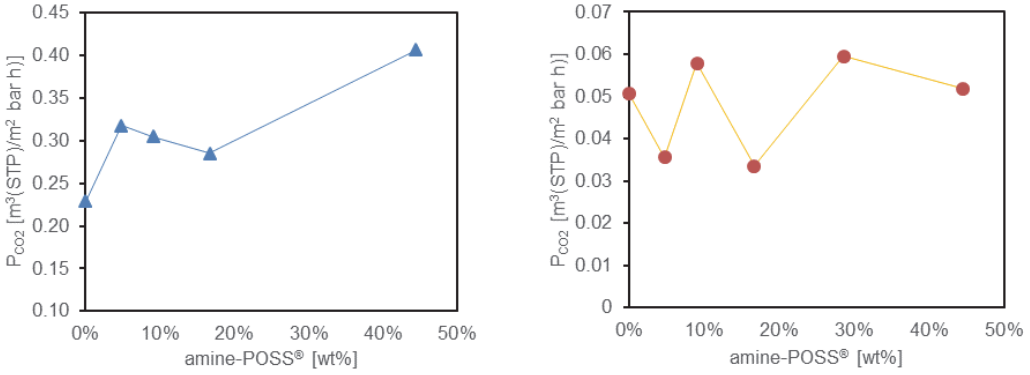

Fig. 9. CO_2 permeance of PVA-amine-POSS® membranes at 100 RH% (left, blue) and 75 RH % (right, orange).

The variation between the two graphs at different relative humidity can be explained by taking into account that there is a certain degree of facilitated transport in the membrane at high RH. In these kind of membranes, the gas transport occurs through both a solution-diffusion and a “carrier-mediated” mechanism, which results in a higher permeation for a specific compound, in this case CO_2.

4.3. SO_2 durability of the PVA-amine-POSS® /PSf membrane

The durability towards SO_2 of the PVA-amine-POSS®/PSf membrane was investigated over a period of 1500 hours under varying SO_2 levels of up to 400 ppm at atmospheric pressure at a temperature of 25 °C. For this test, because it has the best performance, the membrane sample with a PVA:amine-POSS® ratio equal to 1:0.4 was chosen. Fig. 10 and 11 show the $CO_2/N_2/O_2$ permeance and CO_2/N_2 selectivity plotted as a function of time, respectively.

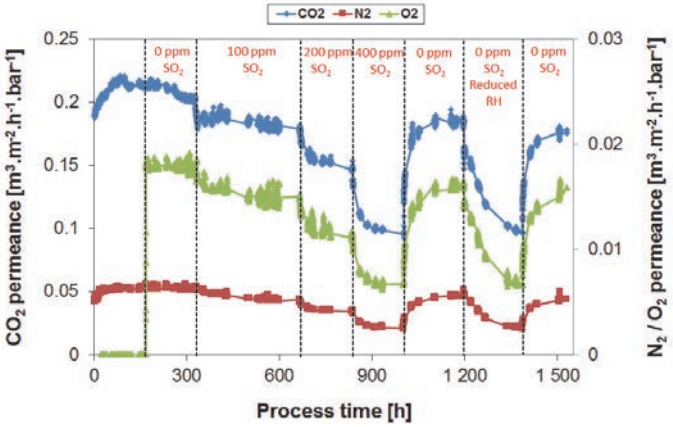

Fig. 10. Effect of SO_2 on the CO_2, N_2 and O_2 permeance

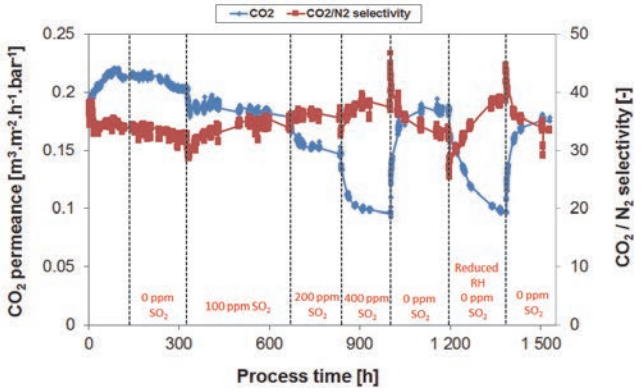

Fig. 11. Effect of SO_2 on the CO_2/N_2 selectivity plotted as function of process time.

A rather stable performance was obtained during the initial 150 hours of testing at a CO_2 permeance and CO_2/N_2 selectivity equal to 0.21 m^3/m^2hbar and 34, respectively. The subsequent introduction of O_2 does not alter the performance substantially, which shows that the membrane is not adversely affected by exposure to O_2 in flue gas. The subsequent introduction of 100 ppm SO_2 (process time of 325h in Fig. 11.), however, results in a decreasing permeance behaviour for all gases, which combined effect and leads to a minor decrease in CO_2/N_2 selectivity. The following increase in SO_2 content to 200 and subsequently 400 ppm results in a further decrease in CO_2 permeance. As the N_2 permeance decreases to a larger extent than the CO_2 permeance, the CO_2/N_2 selectivity of the membrane is actually increasing during the exposure (from ~33 to ~36). However, the decrease in permeance during the SO_2 exposure is explained by the decrease in humidity of the feed gas mixture occurring during the SO_2 exposure. The pre-mixed SO_2/N_2 mixture is added after the bubbling stage of the feed gas to prevent that SO_2 may be absorbed in the water and does not reach the membrane. As a consequence, the humidity of the feed gas is reduced. In the case of the exposure to 400 ppm SO_2 it gives a reduction in RH of 10%. Based on the results presented in Fig. 7, a reduction in the humidity of the feed gas from ~95% to 85% RH could readily result in a decrease in the permeance with 65%. This has experimentally been verified between a process time of 1200 and 1375h, showing that an identical performance is obtained during the 400 ppm SO_2 exposure. After a process time of 1000h, the SO_2 was removed from the feed stream. This results in a gradual recovery in CO_2 permeance between a process time of 1000 and 1200h towards the value obtained prior to any exposure. It shows that SO_2 does not have a permanent negative effect on the membrane performance.

5. Conclusions

This work investigated the addition of amine-POSS® nanoparticles on the CO_2/N_2 separation properties of PVA-based gas separation membranes. Amine-POSS® nanoparticles were obtained via sol-gel process through the hydrolysis of 3-aminopropyltriethoxysilane with a mean particles size of 3 nm. Functionalized nanoparticles – PVA based films were deposited by dip-coating on PSf supports. The SEM cross-section revealed a homogeneous coating on the PSf support and an overall thickness of 3 μm. The CO_2 permeance of the obtained membranes is strongly influenced by the degree of feed gas humidity, since each increment of 25 percentage points in RH increases the permeance by roughly one order of magnitude. The increment of the amount of nanoparticles in the system showed a visible improvement of both permeance and selectivity, however, both parameters tend to plateau after a first increase, which is possibly due to a non-optimal availability of the functional groups at a higher nanoparticles concentration. The CO_2/N_2 selectivity is as highly influenced by relative humidity: at low RH, it is clearly higher, reaching values up to 120. Selectivity increases when amine-POSS® is introduced in the system, but after this first increment, the value appears to be rather stable or decreasing. On the other hand, the permeance does not appear to be significantly influenced by the content of the amine-POSS® nanoparticles at lower humidity, with values oscillating between 0.04 and 0.06 $m^3(STP)/(m^2\ h\ bar)$. However, the performance of the membranes at high humidity is more promising: starting from a value for pure PVA of 0.22, the permeance increases up to 0.4 $m^3(STP)/(m^2\ h\ bar)$. This is a typical behaviour of a FTM membrane where the gas transport occurs through both a solution-diffusion and a “carrier-mediated” mechanism. The durability towards SO_2 of the PVA-amine-POSS®/PSf membrane over a period of 1500 hours under varying SO_2 levels was additionally investigated. The introduction of SO_2 results in a decrease of the permeance for all gases, which combined effect, results in a minor decrease in CO_2/N_2 selectivity. However, this decrease in permeance is explained by the decrease in humidity of the feed gas mixture occurring during the SO_2 exposure. After removal of SO_2 from the feed stream, the membrane showed a gradual recovery in CO_2 permeance, showing that the SO_2 does not have a permanent negative effect on the membrane performance.

Acknowledgements

The research leading to these results has received funding from the European Community's Seventh Framework Program FP7 under grant agreement n° 608555 (HiPerCap). In addition, the support from the Research Council of Norway (RCN) through the CLIMIT program (Project No: 224934) and BIGCCS Centre for Environment-friendly Energy Research (Project No: 193816/S60) are gratefully acknowledged. The contribution of Dr. Sikander Rafik to this paper is also acknowledged.

References

[1] Energy Roadmap 2050 - European Commission – COM (2011) 885, 2011.
[2] IEAGHG. Assessment of emerging CO_2 capture technologies and their potential to reduce costs. 2014/TR4, 2014.
[3] Wee SL, Tye CT, Bhatia. S. Membrane separation process—Pervaporation through zeolite membrane. Sep Purif Technol 2008;63:500-16.
[4] Kim TJ, Vrålstad H, Sandru M, Hägg MB. Separation performance of PVAm composite membrane for CO_2 capture at various pH levels. J Membr Sci 2013;428:218-24.
[5] Wind JD, Paul DR, Koros WJ. Natural gas permeation in polyimide membranes. J Membr Sci 2004;228:227-36.
[6] Hägg MB, Lindbråthen A, He X. Membranes for CO_2 capture – report on pilot plant tests. Advanced Membrane Technology VII. Cork, Ireland. Sept. 11-16, 2016.
[7] Scholes CA, Kentish SE, Stevens GW. Carbon dioxide separation through polymeric membrane systems for flue gas applications. Recent Patents on Chemical Engineering 2008;1:52-66.
[8] Robeson LM. Correlation of separation factor versus permeability for polymeric membranes, J Membr Sci 1991;62:165-85.
[9] Zimmerman CM, Singh A, Koros WJ. Tailoring mixed matrix composite membranes for gas separations, J Membr Sci 1997;137:145-54.
[10] Chung TS, Jiang LY, Li Y, Kulprathipanja S. Mixed matrix membranes (MMMs) comprising organic polymers with dispersed inorganic fillers for gas separation. Progress in Polymer Science 2007;32:483-507.
[11] Kulprathipanja S. Mixed matrix membrane development. Membrane Technology 2002;144:9-12.
[12] Nafisi V, Hägg MB. Development of dual layer of ZIF-8/PEBAX-2533 mixed matrix membrane for CO_2 capture. J Membr Sci 2014;459:244–255.
[13] Sikander F, Deng L, Hägg MB. Role of Facilitated transport Membranes and composite membranes for efficient CO_2 capture – A review. Chem Bio Eng Reviews. 2016;3:68–85.
[14] Kim TJ, Li B, Hagg MB. Novel fixed-site-carrier polyvinylamine membrane for carbon dioxide capture, J. Polym. Sci. B Polym. Phys. 2004;42:4326-4336.
[15] Grandcolas M, Rival N, Landsem E, Simon C. Preparation of POSS-based PVA and PLA nanofibers using needleless electrospinning. Tech J Engin & App Sci 2016;6:24-7.
[16] Deng L, Kim TJ, Hägg MB. Facilitated transport of CO_2 in novel PVAm/PVA blend membrane. J Membr Sci 2009;340:154-63.
[17] Baker RW, Lokhandwala K. Natural Gas Processing with Membranes: An Overview. Ind. Eng. Chem. Res. 2008;47:2109-21.